Original Research Article

NANOBIOMEDICINE

Nanobiomedicine
Volume 5: 1–12
© The Author(s) 2018
Article reuse guidelines:
sagepub.com/journals-permissions
DOI: 10.1177/1849543518794818
journals.sagepub.com/home/nab
SAGE

Nanocomposites containing polyvinyl alcohol and reinforced carbon-based nanofiller: A super effective biologically active material

Khdejah S Hajeeassa[1], Mahmoud A Hussein[1,2], Yasir Anwar[3], Nada Y Tashkandi[1], and Zahra M Al-amshany[1]

Abstract

A new class of biologically active polymer nanocomposites based on polyvinyl alcohol and reinforced mixed graphene/carbon nanotube as carbon-based nanofillers with a general abbreviation (polyvinyl alcohol/mixed graphene–carbon nanotubes) has been successfully synthesized by an efficient solution mixing method with the help of ultrasonic radiation. Mixed graphene and carbon nanotubes ratio has been prepared (50%:50%) wt by wt. Different loading of mixed graphene–carbon nanotubes (2, 5, 10, 15, and 20 wt%) were added to the host polyvinyl alcohol polymer. In this study, polyvinyl alcohol/mixed graphene–carbon nanotubes$_{a–e}$ nanocomposites were characterized and analyzed by X-ray diffraction, Fourier transform infrared, scanning electron microscopy, transmission electron microscopy, and the thermal stability was measured by thermogravimetric analysis and derivative thermal gravimetric. Fourier transform infrared and X-ray diffraction spectra proved the addition of mixed graphene–carbon nanotubes into polyvinyl alcohol matrix. X-ray diffraction patterns for these nanocomposites showed $2\theta = 19.35^\circ$ and 40° due to the crystal nature of polyvinyl alcohol in addition to $2\theta = 26.5^\circ$ which attributed to the graphite plane of carbon-based nanofillers. Thermal stability of polyvinyl alcohol/mixed graphene–carbon nanotubes nanocomposites was enhanced comparing with pure polyvinyl alcohol. The main degradation step ranged between 360° and 450°C. Moreover, maximum composite degradation temperature has appeared at range from 285°C to 267°C and final composite degradation temperature (FCDT) displayed at a temperature range of 469–491°C. Antibacterial property of polyvinyl alcohol/mixed graphene–carbon nanotubes$_{a–e}$ nanocomposites were tested against *Escherichia coli* bacteria using the colony forming units technique. Results showed an improvement of antibacterial property. The rate percentages of polyvinyl alcohol/mixed graphene–carbon nanotubes$_b$, polyvinyl alcohol/mixed graphene–carbon nanotubes$_c$, and polyvinyl alcohol/mixed graphene–carbon nanotubes$_d$ nanocomposites after 24 h are 6%, 5%, and 7% respectively. However, polyvinyl alcohol/mixed graphene–carbon nanotubes$_e$ nanocomposite showed hyperactivity, where its reduction percentage remarkably raised up to 100% which is the highest inhibition rate percentage. In addition, polyvinyl alcohol and polyvinyl alcohol/graphene–carbon nanotubes$_{a–d}$ showed colony forming units values/ml 70×10^6 and $65 \pm 2 \times 10^6$ after 12 h. After 24 h, the colony forming units values/ml were in the range of 86×10^6–95×10^6.

[1] Chemistry Department, Faculty of Science, King Abdulaziz University, Jeddah, Kingdom of Saudi Arabia
[2] Polymer Chemistry Lab. 122, Chemistry Department, Faculty of Science, Assiut University, Assiut, Egypt
[3] Department of Biological Sciences, Faculty of Science, King Abdulaziz University, Jeddah, Saudi Arabia

Corresponding author:
Mahmoud A Hussein, Chemistry Department, Faculty of Science, King Abdulaziz University, P.O. Box 80203, Jeddah 21589, Kingdom of Saudi Arabia.
Emails: mahussein74@yahoo.com; maabdo@kau.edu.sa; mahmali@aun.edu.eg

Creative Commons Non Commercial CC BY-NC: This article is distributed under the terms of the Creative Commons Attribution-NonCommercial 4.0 License (http://www.creativecommons.org/licenses/by-nc/4.0/) which permits non-commercial use, reproduction and distribution of the work without further permission provided the original work is attributed as specified on the SAGE and Open Access pages (https://us.sagepub.com/en-us/nam/open-access-at-sage).

Keywords
Nanocomposites, polyvinyl alcohol, graphene, carbon nanotube, biological interest

Date received: 12 April 2018; accepted: 22 July 2018

Introduction

The nanoscience development in polymeric materials that contain at least one-dimension in nanoscale have enormous attention in science research of advanced materials.[1] Polymer nanocomposite is of great importance among classes of nanocomposite materials. It has been wildly utilized in different fields with a special attention to medicinal and biological applications.[2–4] Physical and engineering properties are improved in the polymer matrix as it gets altered by addition of nanofillers due to of the high surface area to volume ratio.[5] Recently, scientists are focusing on synthesizing polymer nanocomposites for the purposes of use in biological applications.[6] Microorganisms like yeast, bacteria, viruses, and so on, often affect human beings.[7] The effect of polymer nanocomposites on both positive and negative bacteria has been studied in zone of inhibition which successfully shows enhancement in antibacterial activity.[8] In addition, polymer nanocomposites that has an antibacterial effect which can be utilized in food packaging and hygiene products, and longer shelf life.[1,9–11]

Polyvinyl alcohol (PVA) also referred to as PVAL, PVOH, or POVAL is a highly biocompatible, synthetic-nontoxic, and highly water-soluble polymer.[12,13] It can be used as the host of material for composite corresponding to good thermal stability and resistance and are easy to produce.[14] Essentially, PVA can be produced by polymerization from monomer (vinyl acetate) to polyvinyl acetate (PVAc) followed by hydrolysis of acetate of PVAc to PVA.[15] PVA is an environmentally safe product, inexpensive, and is light weight and has good mechanical and optical properties.[16–18] Due to its outstanding chemical and physical properties, PVA can be used in broad applications in different industrial areas such as production of PVA fibers, soil stabilizer, adhesives, textile sizing, biological, industrial, and surgical devices.[19]

Graphene nanoparticles (Gr) with thin two-dimensional, sp^2-hybridized carbon atom and single-layered hexagonal honeycomb structure have drawn attention due to their unique properties, such as its mechanical, thermal, and electrical properties.[20,21] On the other hand, carbon nanotubes (CNTs) which are the rolled-up version of Gr also have important properties, such as, low weight and electrical and thermal conductivity.[22–24] Therefore, both GNP and CNTs have been used as fillers in polymer nanocomposite in different application, for example, sensors, automobiles, capacitors, space ship industries, and biological applications.[25–29]

Recently, Surudžić and coworkers prepared PVA/Gr nanocomposites and showed improvement of mechanical and thermal properties of the polymer as well as high potential for antibacterial activity.[30] Cao et al., demonstrated the effect of different loading of Gr to PVA 1–10% on the antibacterial activity of PVA against *Escherichia coli*; enhancement by 92–97.1% and 92.3–99.7% against *Staphylococcus aureus* were reported.[31] Usman et al. fabricated PVA nanocomposite with graphene oxide/starch/silver as fillers for further investigation in antimicrobial, thermal, and mechanical properties. The prepared films were investigated against *E. coli* and *S. aureus* bacteria and the result showed ascending order in antimicrobial activity by addition (GO/starch/Ag) to PVA matrix.[8] Moreover, increasing number of PVA nanocomposites studies has emerged from fundamental studies to the biological application of nanoscale materials with different nanofillers as reported in the literature.[8,13,15,30,31]

Therefore, a new series of PVA/mixed graphene (MGr)-CNTs nanocomposites are prepared via a simple mixing technique using tetrahydrofuran (THF) as a solvent. PVA and PVA/MGr-CNTs nanocomposites were characterized by Fourier transform infrared (FTIR) and X-ray diffraction (XRD). Also, scanning electron microscopy (SEM) and transmission electron microscopy (TEM) are used to investigate the morphology of these PVA nanocomposites. Thermal behavior of PVA/MGr-CNTs nanocomposites such as thermogravimetric analysis (TGA) and derivative thermogravimetric (DTG) analysis were also discussed. The antibacterial properties of the prepared nanocomposite were evaluated against *E. coli* as Gram negative bacteria and calculate the reduction percentage after 12 and 24 h.

Experimental

Materials

PVA powder with approximate molecular weight = 14,000 g/mol was supplied from PDH. CNTs and Gr nanoplates with 99.5% pure (average length—5–10 μm and diameter—3–10 nm) were purchased from XFNANO advanced materials supplier INC, China. THF with purity = 99.9+%, HPLC grade, purchased from Aldrich, USA, was used as a solvent for nanocomposites fabrication. All the chemicals were used as received without further purification.

Table 1. Chemical composition of the prepared PVA and its related PVA/Gr-CNTs$_{a–e}$ nanocomposites.

Symbols	PVA (g)	Loading MGr-CNTs (50%:50%, g)
Pure PVA	1	—
PVA/MGr-CNTs$_{2\%}$	0.89	0.02
PVA/MGr-CNTs$_{5\%}$	0.95	0.05
PVA/MGr-CNTs$_{10\%}$	0.9	0.1
PVA/MGr-CNTs$_{15\%}$	0.85	0.15
PVA/MGr-CNTs$_{20\%}$	0.8	0.2

PVA: polyvinyl alcohol; MGr: mixed graphene; CNT: carbon nanotube.

Preparation of pure PVA

Pure PVA was prepared in sufficient milliliter of THF by solution casting technique. In a typical procedure, the mixture was sonicated for 30 min at 70°C using an ultrasonic sonicator, followed by stirring for 6 h at 70°C. The solvent of the prepared mixture was evaporated at room temperature in a petri dish for 24 h.

Preparation of PVA/MGr-CNTs nanocomposites

The PVA/MGr-CNTs nanocomposites were prepared by solution mixing method using an ultrasonic sonicator. The nanocomposites samples have been prepared by the following procedures: A known weight of PVA dissolved in THF and sonicated for 15 min at the same temperature. Then, different amount of nanofiller (2, 5, 10, 15, and 20 wt%) from mixed ratio of Gr:CNTs 50%:50% were added to the mixture labeled in Table 1 and continued sonication for an additional 15 min at 70°C in order to prevent coagulation and precipitation. Subsequently, the mixture above was moved to hotplate and stirred for 6 h to improve dispersion. At the end, at room temperature, the solvent was evaporated and was kept for 24 h.

Biological activity

Antibacterial assessment. The antimicrobial properties of the newly prepared PVA/MGr-CNTs$_{a–e}$ nanocomposites were evaluated using colony forming units (CFU) count method. A 5 mL sample of liquid medium (Nutrient Broth) was placed in each test tube, then 0.1 g/mL of PVA/MGr-CNTs$_a$ samples was added to each test tube. After that, 100 µL of *E. coli* O157:H7 was added to each of the test tubes containing liquid medium and incubated for 24 h at 37°C. The samples were successively diluted and then spread over nutrient agar. The samples then were taken at two different timings (12 h and 24 h) for the determination of colonies. A colony counter was used to determine the number of colonies and the experiment was repeated three times to ensure the reliability of results.

Bacterial cell culturing. For the evaluation of antibacterial properties, *E. coli* O157:H7 was chosen as a model, which was provided by King Fahad center, Jeddah. Bacterial cells were grown for antibacterial assessment on nutrient agar (Sigma-Aldrich-70148) containing 1 g/L meat extract, 5 g/L peptones, 2 g/L yeast extract, 2 g/L sodium chloride, and 15 g/L agar in distilled water. Nutrient agar medium plates were prepared, sterilized, and solidified. After solidification bacterial cultures were swabbed on these plates.

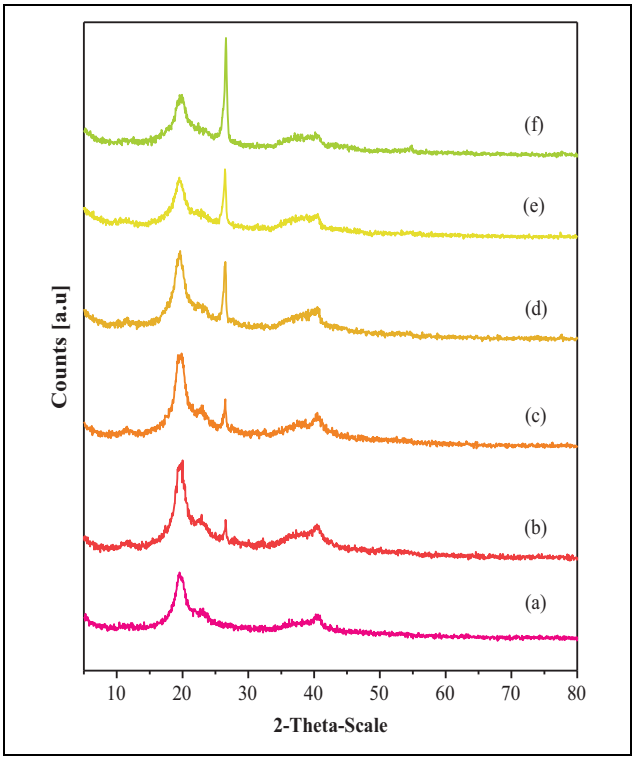

Figure 1. XRD diffraction of (a) PVA and (b–f) PVA/MGr-CNTs$_{a–e}$ nanocomposites. XRD: X-ray diffraction; PVA: polyvinyl alcohol; MGr: mixed graphene; CNT: carbon nanotube.

Characterization method

XRD for neat PVA and PVA/MGr-CNTs was recorded using a Philips powder diffractometer with monochromatic Cu-Kα radiation using the scan step technique in 2θ range of 5° to 80° with a scanning step width of 0.02° and exposition time of 1 s per step, operated at 40 mA and 40 kV. In order to obtain functional groups information of samples, FTIR, a JASCO model, was used. Neat PVA and PVA/MGr-CNTs nanocomposites were analyzed from 450 to 4000 cm^{-1} with 1 cm^{-1} scan rate. Surface morphology images of PVA and PVA/MGr-CNTs nanocomposites were examined. SEM using the JSM-7500F (JEOL-Japan), equipped with Energy Dispersive X-Ray (EDX) Analyzer. TEM micrographs of neat PVA and PVA/MGr-CNTs nanocomposites were taken using the JEOL JEM-1230 TEM. The thermal analysis of PVA/MGr-CNTs nanocomposites was tested and recorded by a TGA and DTG using a TA instrument apparatus model TGA-Q500 using a heating rate of 10°C min^{-1} under nitrogen atmosphere over the

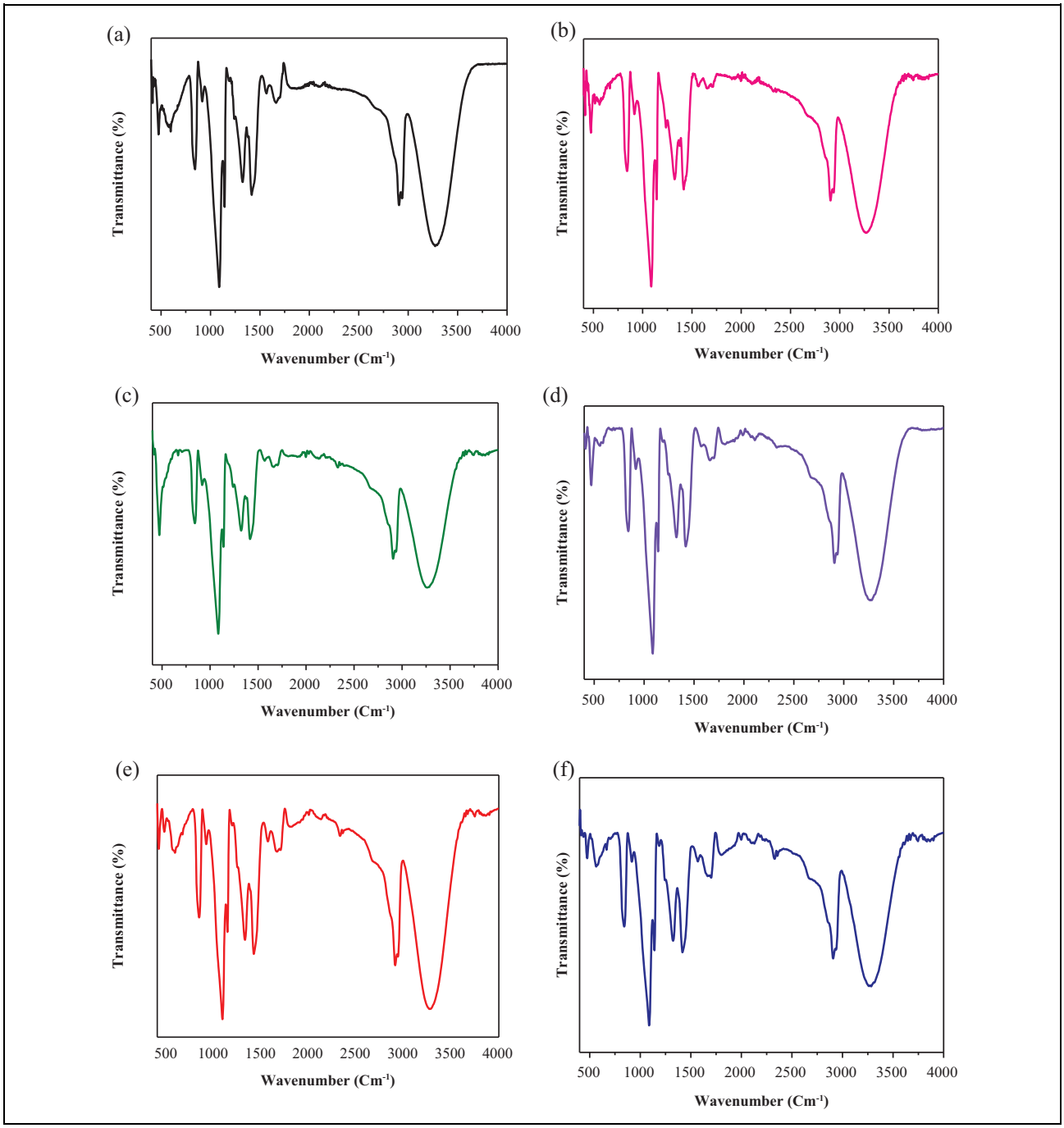

Figure 2. FTIR of (a) PVA and (b–f) PVA/MGR-CNTs$_{a-e}$ nanocomposites. FTIR: Fourier transform infrared; PVA: polyvinyl alcohol; MGr: mixed graphene; CNT: carbon nanotube.

temperature range of 20°C–800°C. The average masses of the samples were 5–10 mg.

Results and discussion

Identification and characterization tools

The potential structure of pure PVA and PVA/MGr-CNTs nanocomposites has been examined by XRD and FTIR characterization techniques.

XRD is often used to investigate the crystallinity of nanocomposite structure as it is a simple and reliable technique,[32] and therefore the XRD for both pure PVA and PVA/MGr-CNTs$_{a-e}$ nanocomposites were recorded. Samples were measured at the range of $2\theta = 5°–80°$. It is well known that pure PVA exhibits a semicrystalline structure due to its high affinity to form hydrogen bond. Figure 1(a) shows two typical peaks diffraction for PVA polymer. The first peak with high intensity appears at $2\theta = 19.35°$ is

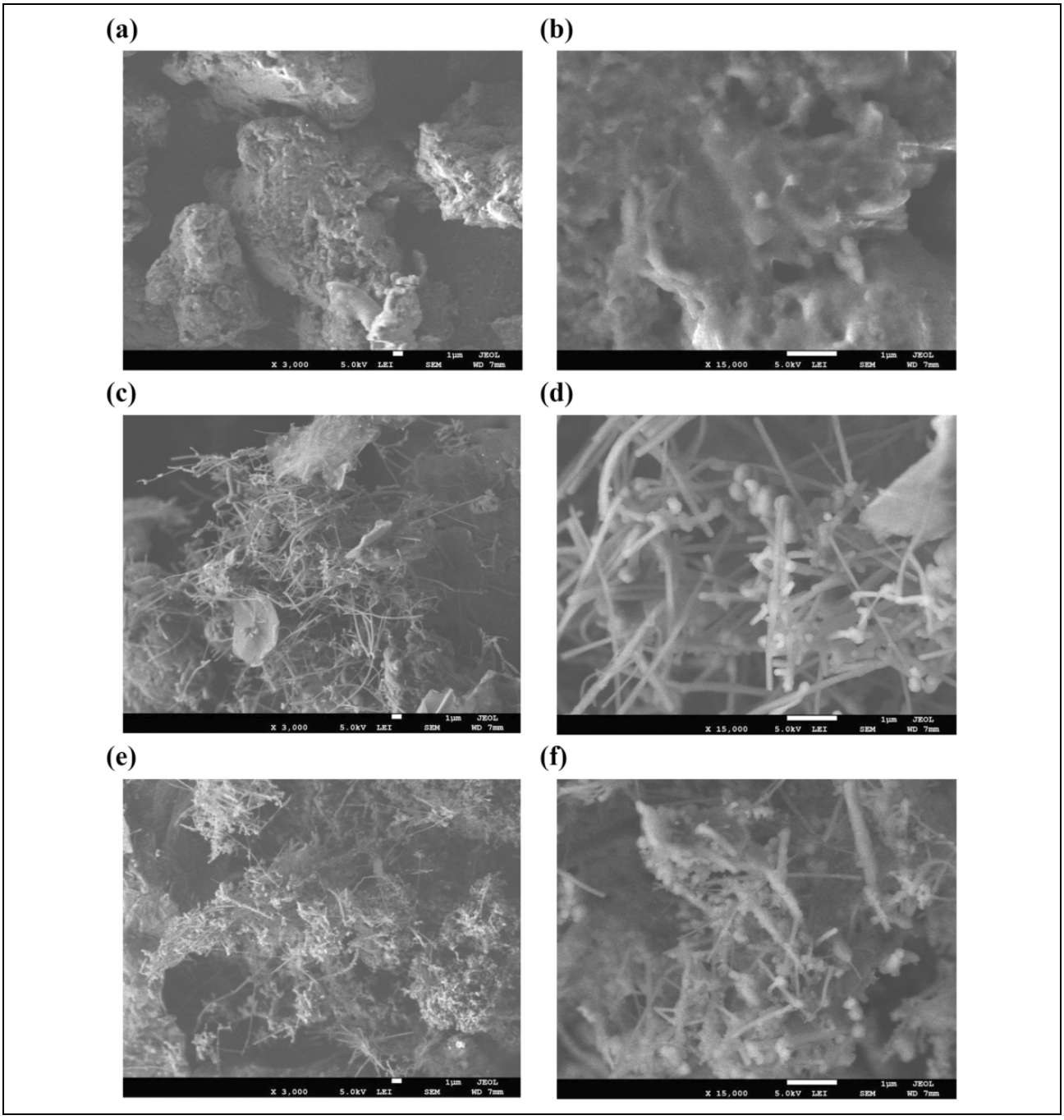

Figure 3. SEM images of PVA at magnifications ((a) X = 3000, (b) X = 15,000), for PVA/MGr-CNTs$_b$ at magnifications ((c) X = 3000 and (d) X = 15,000) and PVA/MGr-CNTs$_e$ at magnifications ((e) X = 3000 and (d) X = 15,000). SEM: scanning electron microscopy; PVA: polyvinyl alcohol; MGr: mixed graphene; CNT: carbon nanotube.

attributed to the (101) crystal plane. The second peak with low intensity at $2\theta = 40^\circ$ is attributed to the semicrystalline nature of PVA.[8,33,34] Figure 1(b) to (f) shows the sharp peak at $2\theta = 26.5^\circ$ (002) for PVA/MGr-CNTs$_{a–e}$ corresponding to the graphite plane which is indicative of the presence of MGr and CNT to PVA matrix. Moreover, increasing the loading of MGr-CNTs results in increasing in the intensity of peaks as illustrated in Figure 1. The shifting of 2θ to the higher value in PVA/MGr-CNTs$_{a–e}$ nanocomposites indicates the crystallinity of PVA matrix reduced by the addition of Gr and CNT nanofillers.[35]

FTIR of pure PVA and PVA/MGr-CNTs are shown in Figure 2. A strong characteristic peak was assigned for the stretching vibration mode of O–H group at 3271.68 and 3286.88 cm^{-1} for PVA and PVA/MGr-CNTs nanocomposites, respectively. For pure PVA, the absorption peak at 1416 cm^{-1} was assigned for PVA. Also, the peak at 2904 cm^{-1} and 2944 cm^{-1} are assigned to C–H stretching in

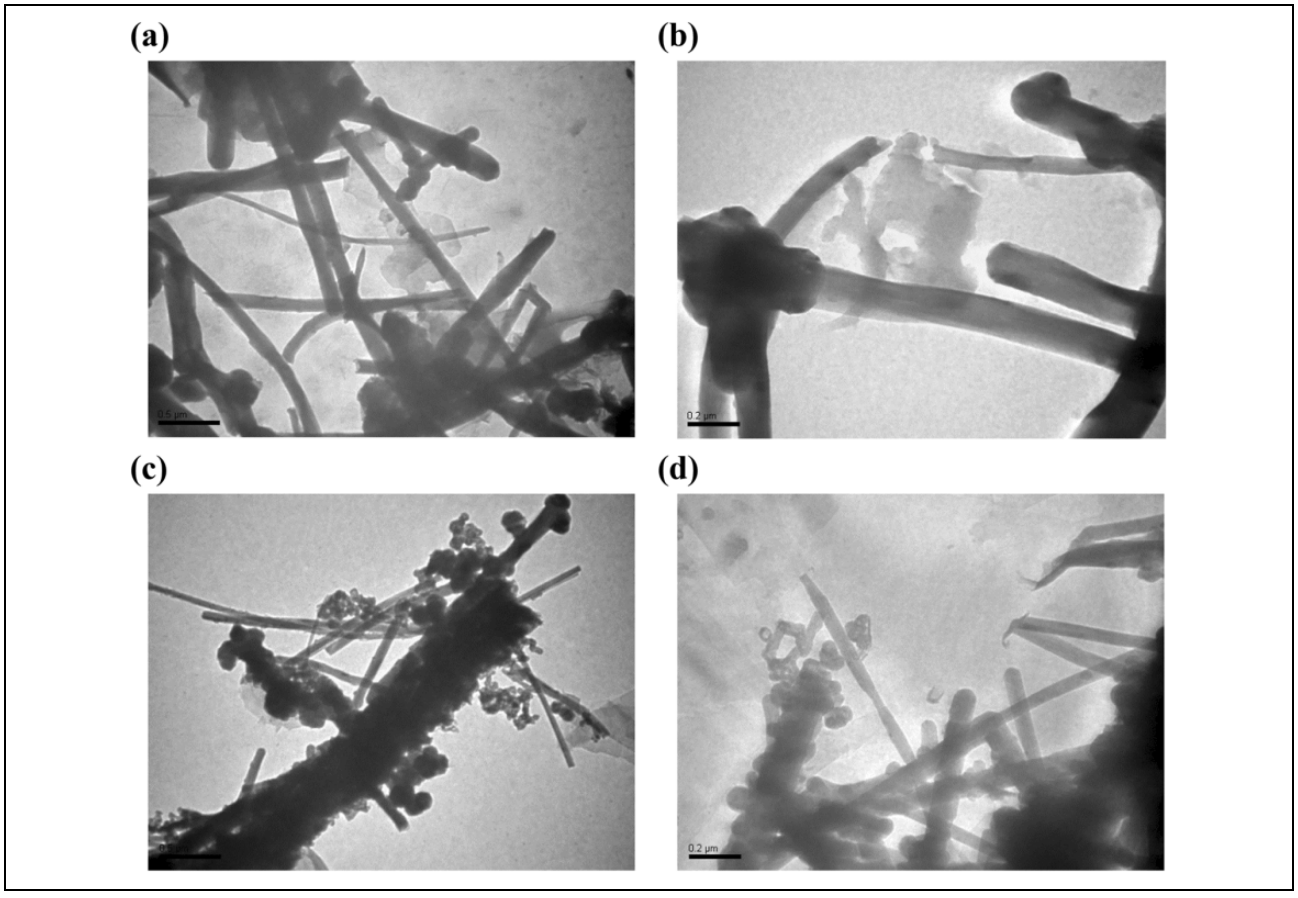

Figure 4. TEM images of PVA/MGr-CNTs$_b$ nanocomposite (a, b) and PVA/MGr-CNTs$_e$ nanocomposite (c, d). TEM: transmission electron microscopy; MGr: mixed graphene; CNT: carbon nanotube.

CH_2 group of PVA backbone and peaks at 1429 and 1093 cm^{-1} are attributed to C–H and C–O bond bending, respectively.[36] The absorption peak at 3570 cm^{-1} was assigned to the hydrogen bond due to hydrophilic forces (intermolecular and intramolecular hydrogen bond) which are plausible through the PVA chains. The absorption peak at wave number 1140 cm^{-1} corresponded to C–C symmetric stretching for PVA and 1143cm^{-1} for PVA/MGr-CNTs nanocomposites. Vibration bands at wave number between 1092 and 1146 cm^{-1} were used as an assessment tool for PVA structure because it is a semicrystalline synthetic polymer able to form some domains depending on several process parameters.[37] A weak peak appeared at 1575 cm^{-1} in Figure 2(b) to (f) for PVA/MGr-CNTs nanocomposites indicative of skeletal vibration of Gr, verifying its presence in PVA nanocomposites matrix. The intense band at 1582 cm^{-1} in PVA nanocomposites spectra is attributed to the sp^2-hybridized C=C vibration of PVA chains.[30] The minor shift of the peaks from 1417 cm^{-1} for PVA to 1416 cm^{-1} for PVA/MGr-CNTs nanocomposites, and C–H peak 1429 cm^{-1} to 1431 cm^{-1} in PVA/MGr-CNTs nanocomposites are attributed to coupling of the –OH in-plane vibration with C–H wagging vibrations and suggest a hydrogen bond interactions between oxygen-containing groups in Gr and CNT and the OH groups in PVA.[30] On the other hand, a decrease in intensity of this absorption band was attributed to the higher loadings of MGr and CNTs which confirm the effect of addition of Gr and CNT on PVA.[38] To summarize, results indicate good dispersion and strong interaction between host PVA and Gr-CNTs nanofillers.

In order to investigate the microstructure and the effects of nanofillers on the dispersion of PVA, SEM, and TEM images of the samples were conducted. The typical surface SEM images for neat PVA and PVA/MGr-CNTs nanocomposites were illustrated in Figure 3. It can be seen that throughout the preparation of PVA nanocomposites, the morphology was changed. Furthermore, SEM images demonstrate that the MGr-CNTs being well-distributed through the PVA matrix. This also indicates that the nanofillers have excellent adhesion and interfacial bonding to PVA. For neat PVA, Figure 3(a) and (b) at magnification X = 3000 and X = 15,000 shows a uniform surface because PVA is semicrystalline in nature. In Figure 3(c) and (d) at magnification X = 3000 and X = 15,000 of PVA/MGr-CNTs$_b$ nanocomposite. Figure 3(e) and (f) shows that PVA/MGr-CNTs$_e$ nanocomposites surfaces are well dispersion of nanofillers and its look becomes straw-like and becomes rougher and assumes a random tangled tubular shape. In

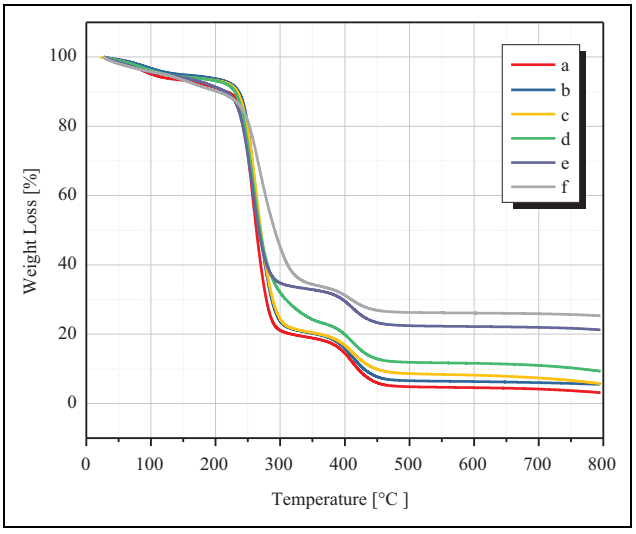

Figure 5. TGA thermograms of (a) pure PVA and (b–f) its compatible PVA/MGr-CNTs$_{a–e}$ nanocomposites. TGA: thermogravimetric analysis; PVA: polyvinyl alcohol; MGr: mixed graphene; CNT: carbon nanotube.

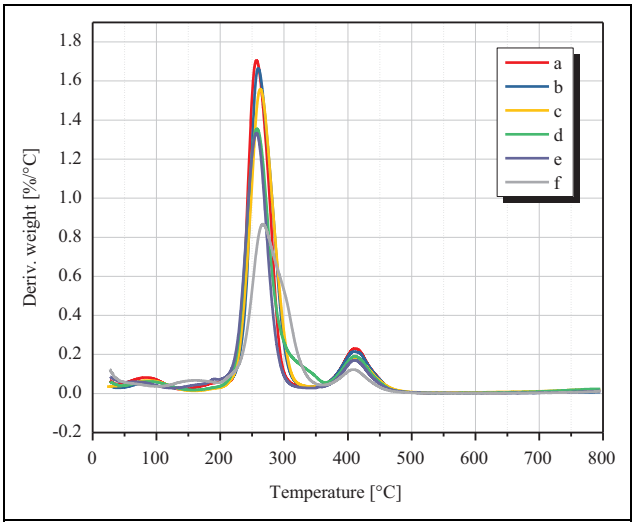

Figure 6. DTG thermograms of (a) pure PVA and (b–f) its compatible PVA/MGr-CNTs$_{a–e}$ nanocomposites. DTG: derivative thermogravimetric; PVA: polyvinyl alcohol; MGr: mixed graphene; CNT: carbon nanotube.

addition, the surface became denser after further addition of Gr-CNTs into the PVA. The strong interfacial interaction is predicted to be caused from hydrogen bonding between hydroxyl groups of the PVA matrix and oxygen-containing groups (hydroxyls, epoxides, and carboxyls) of Gr-CNTs which would cause a positive effect on the mechanical strength of the nanocomposite films.[39]

Further investigation for nanostructure of PVA and PVA nanocomposites using TEM analysis shows the inertial images of the prepared nanocomposites. As selected samples, Figure 4(a) to (d) with scale bar 0.5 and 0.2 μm shows characteristic TEM images for PVA/MGr-CNTs$_{b,e}$ nanocomposites. A good distribution can be seen clearly from the images, due to the high compatibility between PVA and MGr-CNTs. This is attributed to the effect of ultrasonic radiation on the MGr-CNTs of the PVA matrix. The restacked CNTs appear to be wrapped and surrounded by Gr and PVA polymer which is giving the shape like core-shell structure.

It is predictable that the thermal properties of the prepared pure PVA and PVA/MGr-CNTs nanocomposites can be improved considerably by means of high aspect ratio and large interfacial area of nanofillers, good dispersion of Gr and CNT in the PVA host matrix and also the strong interaction between nanofillers and PVA by hydrogen bond and covalent linkage.[40] TGA thermograph and DTG of PVA and PVA nanocomposites have been investigated. Figure 5 presented three noticeable mass loss steps for both pure PVA and PVA/MGr-CNTs$_{a–e}$ nanocomposites, which can be explained by degradation process of the polymer macromolecules. The first step with weight loss at 60–170°C was contributed by evaporation of water molecules, which means decomposition of PVA and the evaporation of the residual solvent. The second step is the weight loss step from 210°C to 316°C which associated to elimination reaction of H_2O molecules. The third step between 360°C and 450°C is due to further decomposition reminders of polyene.[30] On the basis of above results, the thermal stability of PVA nanocomposites is improved via the presence of MGr-CNTs over that of neat PVA. Moreover, the decomposition temperature peak of DTG thermogram illustrated in Figure 6 for pure PVA and PVA/MGr-CNTs$_{a–e}$ nanocomposites. Two peaks appeared and both assigned to the maximum weight loss rate. For nanocomposites, the peak temperature increased comparing with pure PVA.[41] Table 2 shows the temperatures value T_{10}, T_{25}, and T_{50} for 10%, 25%, and 50% weight loss. The weight loss values illustrate at range between 189°C and 291°C. The lowest T_{10} value shows for PVA/MGr-CNTs$_e$ nanocomposite while the highest for PVA/MGr-CNTs$_b$ nanocomposite. Meanwhile, both T_{25} and T_{50} temperatures value for PVA/MGr-CNTs$_d$ shows the lowest and PVA/MGr-CNTs$_e$ shows the highest value.

The maximum composite degradation temperature (CDT_{max})[42–44] indicates two weight losses, the maximum decomposition temperature which is detected from DTG curves presented at Figure 6. For all samples CDT_{max} in Table 2 appears at range 285–267°C. Pure PVA, PVA/MGr-CNTs$_c$, and PVA/MGr-CNTs$_d$ nanocomposites show the same CDT_{max} at 258°C which is the lowest temperature, while PVA/MGr-CNTs$_e$ shows the highest temperature at 267°C. Moreover, Table 2 and Figure 6 reveal the final composite degradation temperature (FCDT)[44,45] which is detected from the TGA curve of all samples. FCDT values display at a temperature range of 469°C–491°C. FCDT shows an increase of temperature with an increase of addition fillers (MGr-CNTs). For pure PVA, FCDT exhibits the lowest value and PVA/MGr-CNTs$_e$. The order of higher CDT_{max} is: PVA/MGr-CNTs$_e$ >

Table 2. Thermal properties of pure PVA and its compatible PVA/MGr-CNTs$_{a–e}$ nanocomposites.

Materials	CDT_{max} (°C)[a]	FCDT (°C)[b]	Temperature (°C) for various percentage decompositions[b]			R_{500} (%)[b]
			T_{10}	T_{25}	T_{50}	
Pure PVA	258	469	209	247	262	4.82
PVA/MGr-CNTs$_a$	260	473	234	253	268	6.56
PVA/MGr-CNTs$_b$	265	480	230	254	269	8.63
PVA/MGr-CNTs$_c$	258	486	227	249	268	11.88
PVA/MGr-CNTs$_d$	258	488	204	246	266	22.44
PVA/MGr-CNTs$_e$	267	491	189	258	291	26.27

PVA: polyvinyl alcohol; MGr: mixed graphene; CNT: carbon nanotube; DTG: derivative thermogravimetric; TGA: thermogravimetric analysis; FCDT: final composite degradation temperature; CDT_{max}: maximum composite degradation temperature.
[a]The values were determined from DTG curves.
[b]The values were determined by TGA at a heating rate of 10°C min^{-1}.

Table 3. Growth conditions and percent inhibition of *E. coli* in the presence of pure PVA, and PVA/MGr-CNTs$_{a–e}$ nanocomposites.

Incubation time (h)	Material used (pure PVA) (CFU/mL)	% Reduction
12	70×10^6	0
24	93×10^6	0
Incubation time (h)	Material used (PVA/MGr-CNTs (2%, CFU/mL)	% Reduction
12	65×10^6	0
24	95×10^6	0
Incubation time (h)	Material used (PVA/MGr-CNTs (5%, CFU/mL)	% Reduction
12	67×10^6	0
24	87×10^6	6
Incubation time (h)	Material used (PVA/MGr-CNTs (10%, CFU/mL)	% Reduction
12	62×10^6	0
24	88×10^6	5
Incubation time (h)	Material Used (PVA/MGr-CNTs (15%, CFU/mL)	% Reduction
12	65×10^6	0
24	86×10^6	7
Incubation time (h)	Material used (PVA/MGr-CNTs (20%, CFU/mL)	% Reduction
12	0×10^6	100
24	0×10^6	100

PVA: polyvinyl alcohol; MGr: mixed graphene; CNT: carbon nanotube; DTG: derivative thermogravimetric; CFU: colony forming units; TGA: thermogravimetric analysis.

PVA/MGr-CNTs$_b$ > PVA/MGr-CNTs$_a$ > PVA/MGr-CNTs$_c$ > PVA/MGr-CNTs$_d$. The thermal stability of PVA composites samples is dependent on the amount of MGr-CNTs dispersed in PVA matrix.

Biological activity

In this work, the count method was used to determine the biological properties of pure PVA and its related PVA/MG-CNTs$_{a–e}$ nanocomposites against *E. coli* as a selected Gram negative bacteria using CFU. The obtained results are illustrated in Table 3 and Figures 7 and 8. Growth characteristic of *E. coli* O157:H7 cell possibility, after treatment with pure PVA, PVA/Gr-CNTs$_{a–e}$. The antibacterial activity of pure PVA and PVA/MGr-CNTs$_{a–e}$ nanocomposites were investigated against *E. coli* shows a significant effectiveness of PVA/MGr-CNTs$_e$ which contained 20% of mixed filler. Figure 7 illustrates the growth of *E. coli* on nutrient plate agar shows inhibition in the presence of pure PVA and PVA/MGr-CNTs$_{a–e}$ nanocomposites. Generally, pure PVA and PVA/Gr-CNTs$_a$ did not show any antibacterial activity in this study. On the other hand, PVA/Gr-CNTs$_b$, PVA/Gr-CNTs$_c$, and PVA/Gr-CNTs$_d$ nanocomposites show more pronounced effect on bacterial growth after 24 h by 6%, 5%, and 7%, respectively. Among them the largest loading of MGr-CNTs (20 wt%) to PVA matrix (PVA/Gr-CNTs$_e$ nanocomposite) shows the highest inhibition rate in the presence of *E.coli* O157:H7. The reduction percentage value is 100% after both 12 and 24 h is clearly observed for this composite as illustrated in Figure 8(a). This enhanced hyperactivity may be attributed to the higher loading of mixed nanofillers within the polymer matrix. Whereas, Figure 8(b) shows viable cell number of *E. coli* after contact with PVA and PVA/MGr-CNTs$_{a–e}$ nanocomposites for 12 and 24 h. These results also confirm the super activity of PVA/Gr-CNTs$_e$ composite compared to the pure PVA and other nanocomposites PVA/Gr-CNTs$_{a–d}$. The CFU values/mL after 12 and 24 h are nearly negligible for PVA/Gr-CNTs$_e$ composite. Whereas, the CFU values per milliliter are 70×10^6 for pure PVA and $65 \pm 2 \times 10^6$ for other nanocomposites after 12 h. After 24 h, PVA and PVA/Gr-CNTs$_{a–d}$ show CFU values/mL in the range of 86×10^6–95×10^6; this can be rationalized as *E. coli* is a Gram negative bacteria that has a complex cell wall comprising two cell membranes and also has a thin peptidoglycan layer.[46] The cell membrane of this bacteria is negatively charged, which may interact with the positively charged Gr and CNTs nanoparticles. This interaction modifies the permeability of the cell membrane by hindering the consumption of nutrients into the cell. Moreover, nanocomposites can produce highly reactive species that is, superoxides, hydrogen peroxide, or hydrogen radicals. The reason is why the

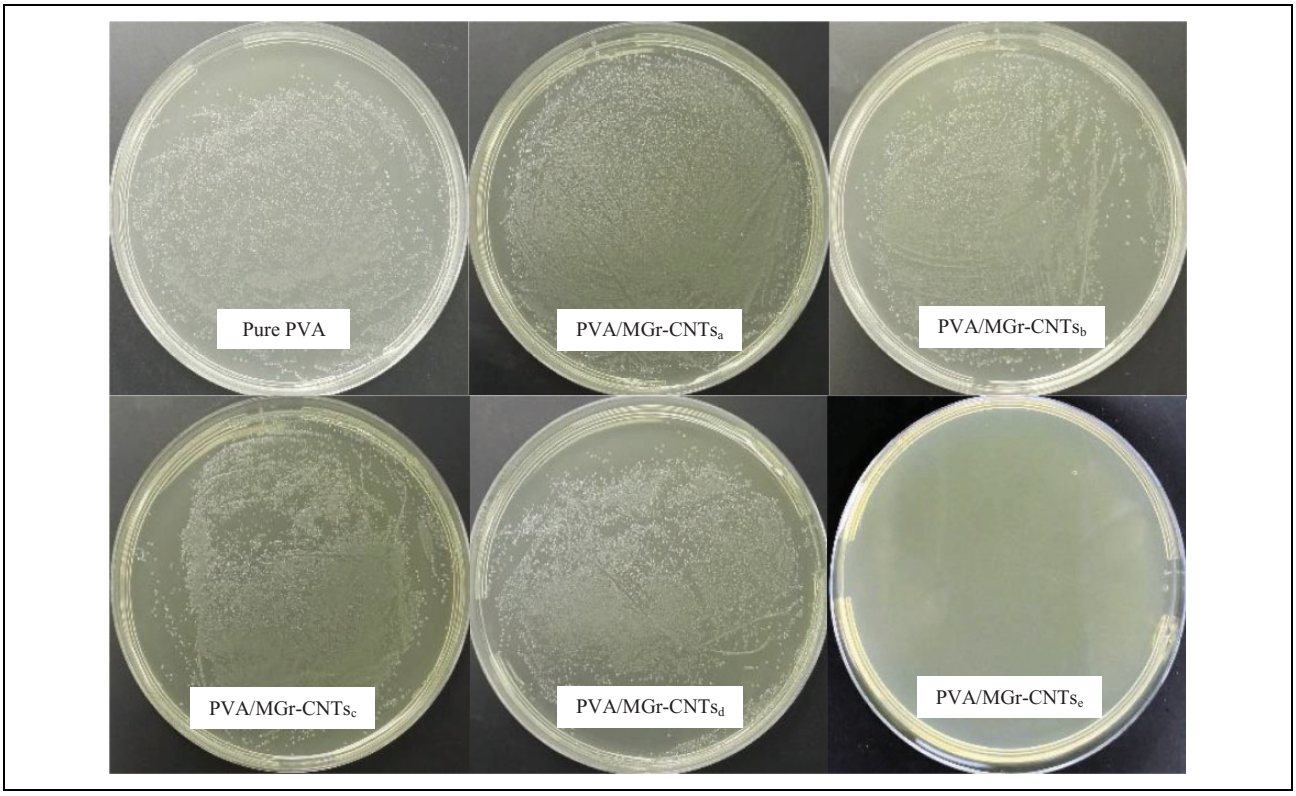

Figure 7. Growth of *E. coli* on nutrient plate agar showing inhibition in the presence of pure PVA and PVA/MGr-CNTs$_{a–e}$ nanocomposites. PVA: polyvinyl alcohol; MGr: mixed graphene; CNT: carbon nanotube; *E. coli*: *Escherichia coli*.

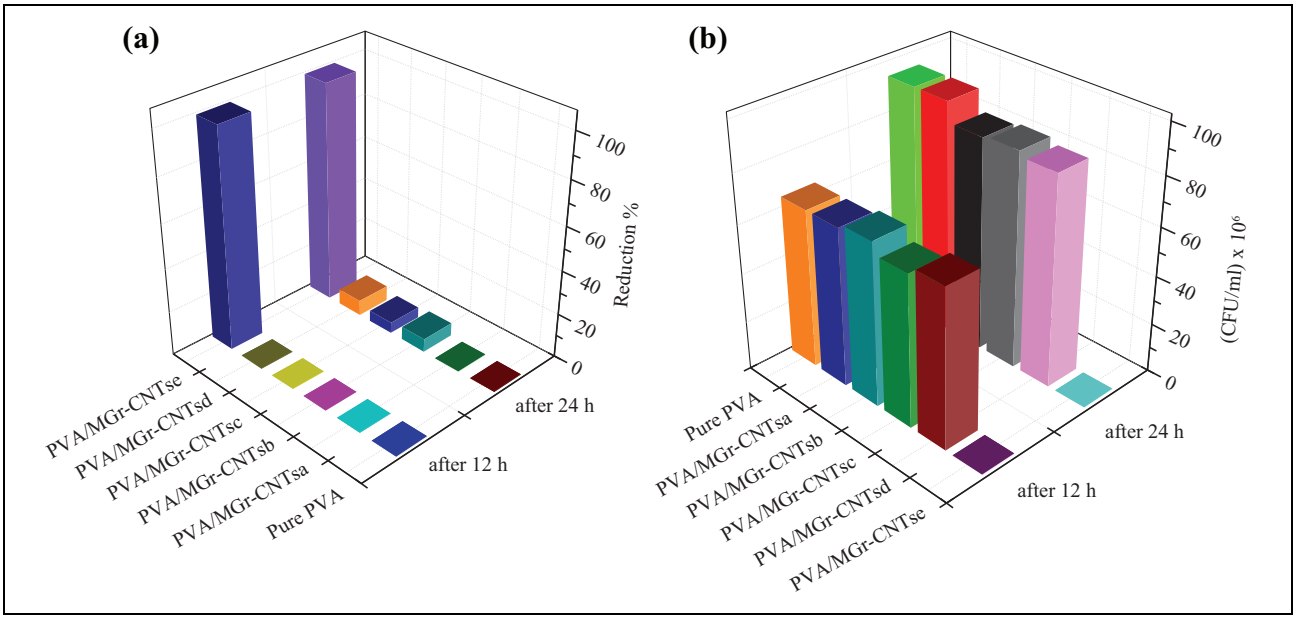

Figure 8. (a) Reduction percentage of *E. coli* after contact with PVA and PVA/MGr-CNTs$_{a–e}$ nanocomposites for 12 and 24 h. (b) Viable cell number of *E. coli* after contact with PVA and PVA/MGr-CNTs$_{a–e}$ nanocomposites for 12 and 24 h. PVA: polyvinyl alcohol; MGr: mixed graphene; CNT: carbon nanotube; *E. coli*: *Escherichia coli*.

viability and growth of these pathogenic bacteria reduced, compared to the pure one. This material can be utilized for waste water treatment as it can absorb water along with *E. coli* and can inhibit its growth in that specific area. Table 4 shows a brief biological screening comparison between variable PVA nanocomposite materials with a special attention to the antibacterial and antifungal activities. Table 4 also shows a clear biological activity (inhibition

Table 4. Biological screening comparison of variable PVA nanocomposites.

PVA nanocomposites	Biological uses	Effects	References
PVA/AgNPs-starch-graphene oxide	Antibacterial activity: *S. aureus* and *E. coli*	Ascending order	Usman et al.[8]
PVA/graphene	Antibacterial activity against *S. aureus* and *E. coli*.	Strong effect	Surudžić et al.[30]
PVA/graphene	Against *E. coli* and *S. aureus*.	97.1–99.7%	Cao et al.[31]
PVA/SWCNT-AgNPs-DNA bio-nanofilm	Antibacterial activity: *E. coli*, *E. faecalis*, *S. aureus*, *B. subtilis*, *S. epidermidis*, *S. typhimurium*, *S. enteric*.	70.91%, 69.31%, 72.89%, 57.78%, 71.76%, 62.85%, 70.52%	Subbiah et al.[47]
PVA/AgNPs	Antibacterial against: *S. aureus*, *B. subtilis*, *E. coli*, *P. aeruginosa*.	11% 17%	Mahmoud[48]
	Antifungal against: *Aspergillus niger* ferm.	18%	
PVA/chitosan-AgNPs	Antibacterial against: Staphylococcus, Micrococcus, *E. coli* and *P. seudomonas*.	Enormous growth inhibition	Vimala et al.[49]
	Antifungal against: *Candida albicans* and Paeruginosa.		
PVA/Ag and PVA/Ag/Gr hydrogel	Antibacterial activity: *S. aureus* and *E. coli*	PVA/Ag: 44.7%, 100% PVA/Ag/Gr: 97%, 100%	Abudabbus et al.[50]
PVA/MGr-CNTs$_e$ nanocomposites	Antibacterial activity: *E. coli*	100%	This work

PVA: polyvinyl alcohol; MGr: mixed graphene; CNT: carbon nanotube; *B. subtilis*: *Bacillus subtilis*; *S. aureus*: *Staphylococcus aureus*; *E. coli*: *Escherichia coli.*

rate—% of reduction) comparison between our prepared materials with other previously reported literature. Data in Table 4 give an evidence for the extreme activity of PVA/MGr-CNTs$_e$ against the selected bacteria.

The antibacterial mechanism of PVA/MGr-CNTs$_{a–e}$ nanocomposites can be rationalized as direct damage on bacterial cell membrane caused by the MGr/CNTs-polymer materials and/or by oxidative stress.[30] Physical damage is also enforced on bacterial membranes upon direct interaction with MGr/CNTs-based materials which result in viability decrease. Particularly, low thickness MGr/CNTs' sharp edges that could cut through the bacteria membranes in an almost blade-like style that causes the release of intracellular substances.[51,52]

MGr/CNTs may also chemically increase cellular oxidative stress, which could interrupt a certain microbial process. Reactive oxygen species (ROS) can also be produced by Gr, graphene oxide, or reduced graphene oxide from the MGr/CNTs-based materials, which can cause oxidative stress on the bacterial cell. Another possibility is that MGr/CNT-based materials may disturb a certain microbial process or a vital cellular component or structure by distressing or oxidizing them, but without generating ROS. The suggested effects above are increased for the reduced form of these carbon-based nanofiller (MGr/CNT) due to better charge transfer between the Gr-based material and the bacteria and/or stronger contact between bacteria's cell membrane and the sharp sheet edges.[51] Nevertheless, the antibacterial activity of MGr-CNTs is still debatable; therefore, the antibacterial activity mechanism of MGr/CNTs should be further investigated. These results are in line with the obtained FTIR, XRD, SEM, and TEM results and support our hypothesis that MGr-CNTs was uniformly dispersed on PVA matrix. The strikingly increased antimicrobial activity of PVA/MGr-CNTs$_{a–e}$ nanocomposites could be due to the synergistic effects of MGr-CNTs and PVA matrix.

Conclusions

In this study, polymer nanocomposites in the form of PVA/MGr-CNTs$_{a–e}$ have been successfully prepared via simple casting method with control loading of MGr-CNTs to the PVA polymer matrix. The investigation of the effects and changes in thermal and biological properties of PVA after an addition of nanofillers (MGr-CNTs). Samples have been characterized by XRD and FTIR and the results indicate that a uniform incorporation of PVA into Gr-CNTs due to the new covalent linkage between them. SEM and TEM analysis also showed the complete homogenously dispersion of MGr-CNTs into PVA matrix. TGA and DTG results clarified that the thermal stability of PVA nanocomposites were also significantly enhanced with addition of even a few loadings of MGr and CNTs. The lowest thermal stability was found in PVA/Gr-CNTs$_a$ while the highest was PVA/MGr-CNTs$_e$ nanocomposite. Pure PVA, PVA/MGr-CNTs$_c$, and PVA/MGr-CNTs$_d$ nanocomposites show the nearly identical CDT_{max} temperatures at 258°C, while PVA/MGr-CNTs$_e$ shows the highest temperature at 267°C. FCDT shows an increase of temperature with an increase of addition fillers (MGr-CNTs). The order of higher CDT_{max} is found as follows: PVA/MG-CNTs$_e$ > PVA/MG-CNTs$_b$ > PVA/MG-CNTs$_a$ > PVA/MG-CNTs$_c$ > PVA/MG-CNTs$_d$. The prepared PVA/MGr-CNTs$_{a–e}$ nanocomposites were tested for antibacterial activity against *E. coli* bacteria. CFU values/mL after 12 h are 70×10^6 for pure PVA and $65 \pm 2 \times 10^6$ for other nanocomposites. After 24 h, PVA and PVA/Gr-CNTs$_{a–d}$ show CFU values/mL in the range of 86×10^6–95×10^6. PVA/MGr-CNTs$_e$ nanocomposite showed the highest inhibition

(100%) compared to the pure PVA and other prepared nanocomposites.

Declaration of Conflicting Interests

The author(s) declared no potential conflicts of interest with respect to the research, authorship, and/or publication of this article.

Funding

The author(s) received no financial support for the research, authorship, and/or publication of this article.

ORCID iD

Mahmoud A Hussein http://orcid.org/0000-0002-5128-5136

References

1. Ghaffari-Moghaddam M and Eslahi H. Synthesis, characterization and antibacterial properties of a novel nanocomposite based on polyaniline/polyvinyl alcohol/Ag. *Arabian J Chem* 2014; 7(5): 846–855.
2. Sabaa MW, Abdallah HM, Mohamed NA, et al. Synthesis, characterization and application of biodegradable crosslinked carboxymethyl chitosan/poly (vinyl alcohol) clay nanocomposites. *Mater Sci Eng C* 2015; 56: 363–373.
3. Abdul Khalil HPS, Saurabh CK, Adnan AS, et al. A review on chitosan-cellulose blends and nanocellulose reinforced chitosan biocomposites: properties and their applications. *Carbohydr Polym* 2016; 150: 216–226.
4. Shahadat M, Teng TT, Rafatullah M, et al. Titanium-based nanocomposite materials: a review of recent advances and perspectives. *Colloids Surf B Biointerfaces* 2015; 126: 121–137.
5. Alateyah AI, Dhakal HN, Zhang ZY, et al. Low velocity impact and creep-strain behaviour of vinyl ester matrix nanocomposites based on layered silicate. *Int J Polym Sci* 2014; 2014: 1–10.
6. Huang YU, Wang D, Zhu X, et al. Synthesis and therapeutic applications of biocompatible or biodegradable hyperbranched polymers. *Polym Chem* 2015; 6(15): 2794–2812.
7. Yu D-G, Teng M-Y, Chou W-L, et al. Characterization and inhibitory effect of antibacterial PAN-based hollow fiber loaded with silver nitrate. *J Memb Sci* 2003; 225(1): 115–123.
8. Usman A, Hussain Z, Riaz A, et al. Enhanced mechanical, thermal and antimicrobial properties of poly (vinyl alcohol)/graphene oxide/starch/silver nanocomposites films. *Carbohydr Polym* 2016; 153: 592–599.
9. De Azeredo HMC. Nanocomposites for food packaging applications. *Food Res Int* 2009; 42(9): 1240–1253.
10. Markarian J. Antimicrobials find new healthcare applications. *Plast Additives Compounding* 2009; 11(1): 18–22.
11. Xu J, Hu Y, Song L, et al. Preparation and characterization of poly (vinyl alcohol)/graphite oxide nanocomposite. *Carbon* 2002; 40(3): 450–451.
12. Finch CA. *Polyvinyl alcohol; properties and applications*. New York, USA: John Wiley & Sons, 1973.
13. Georgieva N, Bryaskova R, and Tzoneva R. New Polyvinyl alcohol-based hybrid materials for biomedical application. *Mater Lett* 2012; 88: 19–22.
14. Lei P, Wang F, Gao X, et al. Immobilization of TiO_2 nanoparticles in polymeric substrates by chemical bonding for multi-cycle photodegradation of organic pollutants. *J Hazard Mater* 2012; 227–228: 185–194.
15. Horikoshi T, Ogawa A, Saito T, et al. Properties of Polyvinylalcohol fiber as reinforcing materials for cementitious composites. In: Fischer G and Li VC (eds) *International RILEM workshop on HPFRCC in structural applications*. Paris, France: RILEM Publications SARL, 2006, pp. 145–153.
16. Hemalatha KS, Rukmani K, Suriyamurthy N, et al. Synthesis, characterization and optical properties of hybrid PVA–ZnO nanocomposite: a composition dependent study. *Mater Res Bull* 2014; 51: 438–446.
17. Lou Y, Liu M, Miao X, et al. Improvement of the mechanical properties of nano-TiO_2/poly (vinyl alcohol) composites by enhanced interaction between nanofiller and matrix. *Polym Compos* 2010; 31(7): 1184–1193.
18. Mallakpour S and Dinari M. Nanocomposites of poly (vinyl alcohol) reinforced with chemically modified Al_2O_3: synthesis and characterization. *J Macromolecular Sci Part B* 2013; 52(11): 1651–1661.
19. Thong CC, Teo DCL, and Ng CK. Application of polyvinyl alcohol (PVA) in cement-based composite materials: a review of its engineering properties and microstructure behavior. *Constr Build Mater* 2016; 107: 172–180.
20. Ansari MO, Yadav SK, Cho JW, et al. Thermal stability in terms of DC electrical conductivity retention and the efficacy of mixing technique in the preparation of nanocomposites of graphene/polyaniline over the carbon nanotubes/polyaniline. *Compos B Eng* 2013; 47: 155–161.
21. Wang L, Wu Y, Chen F, et al. Photocatalytic enhancement of Mg-doped ZnO nanocrystals hybridized with reduced graphene oxide sheets. *Prog Nat Sci Mat Int* 2014; 24(1): 6–12.
22. Ansari MO, Khan MM, Ansari SA, et al. pTSA doped conducting graphene/polyaniline nanocomposite fibers: Thermoelectric behavior and electrode analysis. *Chem Eng J* 2014; 242: 155–161.
23. Rafiee MA. Graphene-based composite materials, PhD Thesis, Troy, New York, USA: Rensselaer Polytechnic Institute, 2011.
24. Robinson JT, Perkins FK, Snow ES, et al. Reduced graphene oxide molecular sensors. *Nano Lett* 2008; 8(10): 3137–3140.
25. Ansari MO and Mohammad F. Thermal stability and electrical properties of dodecyl-benzene-sulfonic-acid doped nanocomposites of polyaniline and multi-walled carbon nanotubes. *Compos B Eng* 2012; 43(8): 3541–3548.
26. Broza G, Piszczek K, Schulte K, et al. Nanocomposites of poly (vinyl chloride) with carbon nanotubes (CNT). *Compos Sci Technol* 2007; 67(5): 890–894.
27. Moniruzzaman M and Winey KI. Polymer nanocomposites containing carbon nanotubes. *Macromolecules* 2006; 39(16): 5194–5205.

28. Ramanathan T, Abdala AA, Stankovich S, et al. Functionalized graphene sheets for polymer nanocomposites. *Nat Nanotechnol* 2008; 3(6): 327–331.
29. Stankovich S, Dikin DA, Dommett GH, et al. Graphene-based composite materials. *Nature* 2006; 442(7100): 282–286.
30. Surudžić R, Janković A, Mitrić M, et al. The effect of graphene loading on mechanical, thermal and biological properties of poly (vinyl alcohol)/graphene nanocomposites. *J Ind Eng Chem* 2016; 34: 250–257.
31. Cao YC, Wei W, Liu J, et al. The preparation of graphene reinforced poly (vinyl alcohol) antibacterial nanocomposite thin film. *Int J Polym Sci* 2015; 2015: 1–7.
32. Mallakpour S, Zhiani M, Barati A, et al. Improving the direct methanol fuel cell performance with poly (vinyl alcohol)/titanium dioxide nanocomposites as a novel electrolyte additive. *Int J Hydrogen Energy* 2013; 38(28): 12418–12426.
33. Huang S-J, Lee H-K, and Kang W-H. Proton conducting behavior of a novel composite based on Phosphosilicate/Poly (vinyl alcohol). *J Korean Ceram Soc* 2005; 42(2): 77–80.
34. Krumova M, Lopez D, Benavente R, et al. Effect of crosslinking on the mechanical and thermal properties of poly (vinyl alcohol). *Polymer* 2000; 41(26): 9265–9272.
35. Tang Z, Lei Y, Guo B, et al. The use of rhodamine B-decorated graphene as a reinforcement in polyvinyl alcohol composites. *Polymer* 2012; 53(2): 673–680.
36. Malikov EY, Muradov MB, Akperov OH, et al. Synthesis and characterization of polyvinyl alcohol based multiwalled carbon nanotube nanocomposites. *Physica E Low Dimens Syst Nanostruct* 2014; 61: 129–134.
37. Srikanth C, Sridhar BC, Prasad M, et al. Characterization and DC conductivity of novel ZnO doped polyvinyl alcohol (PVA) nano-composite films. *J Adv Phys* 2016; 5(2): 105–109.
38. Jose J, Al-Harthi MA, AlMa'adeed MA, et al. Effect of graphene loading on thermomechanical properties of poly (vinyl alcohol)/starch blend. *J Appl Polym Sci* 2015; 132: 4 1827.
39. Ma H-L, Zhang L, Zhang Y, et al. Radiation preparation of graphene/carbon nanotubes hybrid fillers for mechanical reinforcement of poly (vinyl alcohol) films. *Radiat Phys Chem* 2016; 118: 21–26.
40. Yuan X. Enhanced interfacial interaction for effective reinforcement of poly (vinyl alcohol) nanocomposites at low loading of graphene. *Polym Bulletin* 2011; 67(9): 1785–1797.
41. Liang J, Huang Y, Zhang L, et al. Molecular level dispersion of graphene into poly (vinyl alcohol) and effective reinforcement of their nanocomposites. *Adv Funct Mat* 2009; 19(14):2297–2302.
42. Abu-Zied BM, Hussein MA, and Asiri AM. The role of eliminating PEG from PEG/MCM-41 composite on the structural, textural and electrical conductivity properties of MCM-41. *Int J Electrochem Sci* 2015; 10: 1372–1383.
43. Hussein MA, El-Shishtawy RM, and Obaid AY. The impact of graphene nano-plates on the behavior of novel conducting polyazomethine nanocomposites. *RSC Adv* 2017; 17: 9998–10008.
44. Alosaimi AM, Hussein MA, Abdelaal MY, et al. Polysulfones based modified organoclay nanocomposites as a promising breast anticancer agent. *Cogent Chem* 2017; 3(1): 1417672.
45. Hussein MA, El-Shishtawy RM, Obaid AY, et al. Influence of single-walled carbon nanotubes on the performance of poly(azomethine-ether) composite materials. *Polym Plast Technol Eng* 2018, 57(11): 1150–1163.
46. Lichter JA and Rubner MF. Polyelectrolyte multilayers with intrinsic antimicrobial functionality: the importance of mobile polycations. *Langmuir* 2009; 25(13): 7686–7694.
47. Subbiah RP, Lee H, Veerapandian M, et al. Structural and biological evaluation of a multifunctional SWCNT-AgNPs-DNA/PVA bio-nanofilm. *Anal Bioanal Chem* 2011; 400(2): 547–560.
48. Mahmoud KH. Synthesis, characterization, optical and antimicrobial studies of polyvinyl alcohol–silver nanocomposites. *Spectrochim Acta A Mol Biomol Spectrosc* 2015; 138: 434–440.
49. Vimala K, Yallapu MM, Varaprasad K, et al. Fabrication of curcumin encapsulated chitosan-PVA silver nanocomposite films for improved antimicrobial activity. *J Biomater Nanobiotechnol* 2011; 2(01): 55.
50. Abudabbus MM, Jevremović I, Janković A, et al. Biological activity of electrochemically synthesized silver doped polyvinyl alcohol/graphene composite hydrogel discs for biomedical applications. *Compos B Eng* 2016; 104: 26–34.
51. Liu S, Zeng TH, Hofmann M, et al. Antibacterial activity of graphite, graphite oxide, graphene oxide, and reduced graphene oxide: membrane and oxidative stress. *ACS Nano* 2011; 5(9): 6971–6980.
52. Santos CM, Mangadlao J, Ahmed F, et al. Graphene nanocomposite for biomedical applications: fabrication, antimicrobial and cytotoxic investigations. *Nanotechnology* 2012; 23(39): 395101.